



SEISMIC DESIGN OF DUCTILE LINKED ROCKING STEEL FRAMES

F. Z. Wang⁽¹⁾, Y. Cui⁽²⁾

⁽¹⁾ Ph.D. Candidate, Faculty of Infrastructure Engineering, Dalian University of Technology, Dalian, China, wang-fz@mail.dlut.edu.cn

⁽²⁾ Associate Professor, State Key Laboratory of Coastal and Offshore Engineering, Dalian University of Technology, Dalian, China, cuiyao@dlut.edu.cn

Abstract

The ductile linked rocking steel frames (DLRF) has been developed which can eliminate residual drifts and concentrate major damage in structural fuses. The DLRF consists of three main components. The rocking steel braced frames are allowed to uplift and rock at the rocking column bases in response to earthquakes, so that the deformation is distributed uniformly along with the building height and the soft-story collapse mechanism could be prevented. The ductile links are used to connect pairs of the rocking steel braced frames and thus the seismic energy is dissipated during relative movement between the frames. It will also facilitate post-disaster recovery back towards re-occupancy and reduce the operational downtime by being bolted to the rocking steel braced frames. The rocking column bases permit the column bottom uplift and recenter, accompanied by supplemental energy dissipation devices to minimize the loads acted on the primary structural elements. In addition, the rocking column bases are designed to resist horizontal shear forces while the column uplift. The performance objectives corresponding to various earthquake intensities for each limit state are investigated based on the overturning moment-roof drift relationship of the DLRF. From the service level earthquake (SLE, with a probability of exceedance of 63% in 50 years) to the design basis earthquake (DBE, with a probability of exceedance of 10% in 50 years), all the structural elements remain elastic and the DLRF reaches the immediate occupancy (IO) level, accompanied by the onset of rocking. From the DBE to the maximum considered earthquake (MCE, with a probability of exceedance of 2% in 50 years), yielding of the ductile links is observed during this stage and the rapid return (RR) level is achieved. As exceeding the MCE and even up to the very rare earthquake (VRE, with a probability of exceedance of 0.5% in 50 years), the rocking column bases begin to yield while the rocking steel braced frame elements still remain elastic, and thereby intending to achieve collapse prevention (CP) level. Then the associated design procedure to describe the overturning moment-roof drift under various ground motion intensities are established. The ability of the design methodology to achieve the specified performance objectives is validated by applying it to a case study of a four-story residential building. Based on the results of the nonlinear static analyses, the ability to damage control and prediction of the failure mechanism was demonstrated for the proposed DLRF.

Keywords: rocking steel frames, ductile links, rocking column bases, performance objectives, seismic design



1. Introduction

For most buildings designed in accordance with current seismic codes, the input earthquake energy is mainly dissipated by primary structural components in the lateral force-resisting systems under design basis earthquake (DBE, with a probability of exceedance of 10% in 50 years). Although it can effectively prevent the building from collapse, the damage and the residual deformation of key components become inevitable. For a community, the disruption of structural functions may bring serious negative impacts on the post-earthquake recovery, for instance, the 2011 Tohoku earthquake and 2011 Christchurch earthquake in New Zealand [1, 2]. In recent years, the development of resilient systems has provided an effective idea for improving the seismic community resilience.

As an alternative resilient system, the rocking system can control the distribution of the drift over the height of the building through rigid body rotation, and mitigate the damage of primary structural elements caused by the soft-story failure. The favorable effect of releasing the constraint between the column and the foundation on structures was found by Housner [3]. This paper is mainly focused on rocking steel frames. Previous studies on rocking steel frames indicated that the input seismic energy is dissipated by the relative deformation of the rocking interface instead of being absorbed by the structural elements in frames [4-6]. Several innovative technologies have been introduced to rocking steel frames, such as post-tensioning strands which provide self-centering force to recenter the frame and energy-dissipating fuses which improve the energy dissipation capacity of the frame [7-11]. This type of frame was known as controlled rocking steel frames. In recent years, both performance-based seismic design methodology and capacity design procedure for controlled rocking steel frames have been proposed and validated by some researchers [12-13].

One characteristic of these systems is that post-tensioning strands are used to provide restoring forces and resistance against overturning. However, the initial stress required for PT strands may be relatively high especially for taller frames which in turn may bring additional precompression acting force on the frame. It may be detrimental to the whole stability of the rocking frame. The other characteristic is that the uplifting column bases are just placed on the foundation without any constraints in the vertical direction, which may lead to global uplift easily.

In this paper, a modified steel rocking frame that does not use the PT strands to recenter the frame was developed. The self-centering force is provided by the gravity load of the steel braced frames, together with the rocking column bases which was particularly designed to resist both the tension and compression force. The inelastic deformation is confined to the rocking column bases and the ductile links, which may significantly mitigate major structural elements damage and reduce residual drifts after an earthquake. Based on the hysteretic response of the DLRF under cyclic lateral loads, a capacity design procedure was developed and validated by using a four-story prototype structure.

2. System Behavior of the DLRF

2.1 Configuration of the DLRF

The configuration of the DLRF is illustrated in Fig. 1, comprising three main components:

- (1) Two rocking steel braced frames, in which the steel columns are permitted to separate from the foundation and return back to vertical position when subjected to cyclic lateral loads. The rocking steel braced frames are able to create a uniform inter-story drift over the height and prevent soft-story collapse mechanism by rocking like a rigid body in response to earthquakes. The primary structural elements, including columns, beams, and braces, are expected to remain essentially elastic.
- (2) Ductile links, by which pairs of rocking steel braced frames are coupled, and thus the seismic energy is dissipated during relative movement between the frames. It will also facilitate post-disaster recovery back towards re-occupancy and reduce the operational downtime by being bolted to the rocking steel braced frames.



(3) Rocking column bases, which permits the column bottom uplift and recenter, accompanied by supplemental energy dissipation devices to minimize the loads acted on the primary structural elements. In addition, the rocking column bases are designed to resist horizontal shear forces while the column uplift.

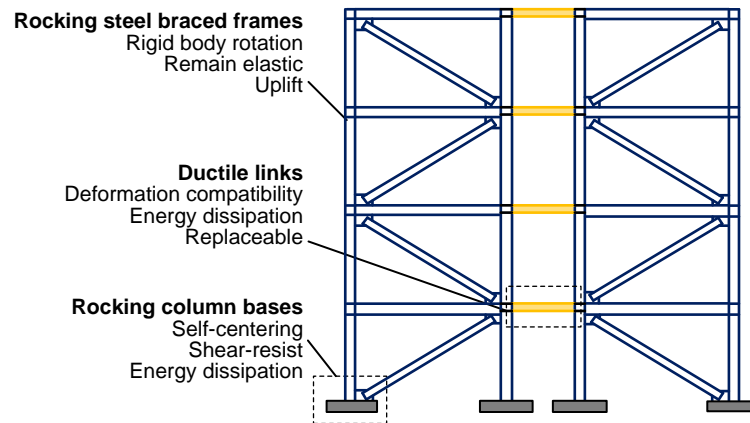
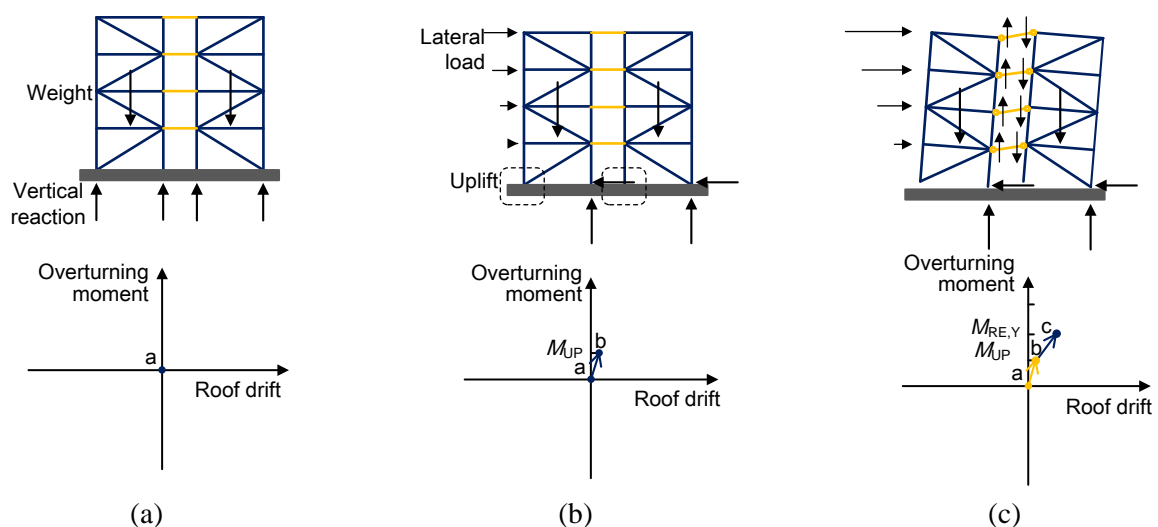


Fig. 1 – Configuration of the ductile linked rocking steel frames

The various stages of the DLRF response to lateral forces in forward and reverse direction are illustrated in Fig. 2, together with the associated overturning moment-roof drift relationship of the DLRF. At the beginning (step a), the DLRF at rest and is balanced by its gravity load. As the lateral load increases (step b), the initial gravity is overcome until the vertical force on one column bottom of the rocking steel braced frames reaches zero. This marks the initiation of rocking and the behavior of the DLRF is consistent with that of the traditional steel braced frame up to this point, corresponding to a sudden change in the initial loading stiffness.

The next event is the rocking of the steel braced frames, which work together through the ductile links. During this stage, a gap is formed between the column bottom and the foundation surface. This continues until the ductile links begin to yield (step c), accompanied by a change in the loading stiffness at this point. With the increment of lateral load, the ductile links that yielded at the end of step c continue to resist lateral load. The next event is the yielding of the rocking column bases (step d). This continues until unloading occurs (step e) and is followed by a reversal loading and unloading (steps f to g). For the symmetrical structural systems, the relationship between the overturning moment and the relative roof drift in the reverse direction is identical to that in the forward direction (step h). After removal of the lateral load, the DLRF returns to its original state without residual drift, as illustrated in Fig. 2 (h).



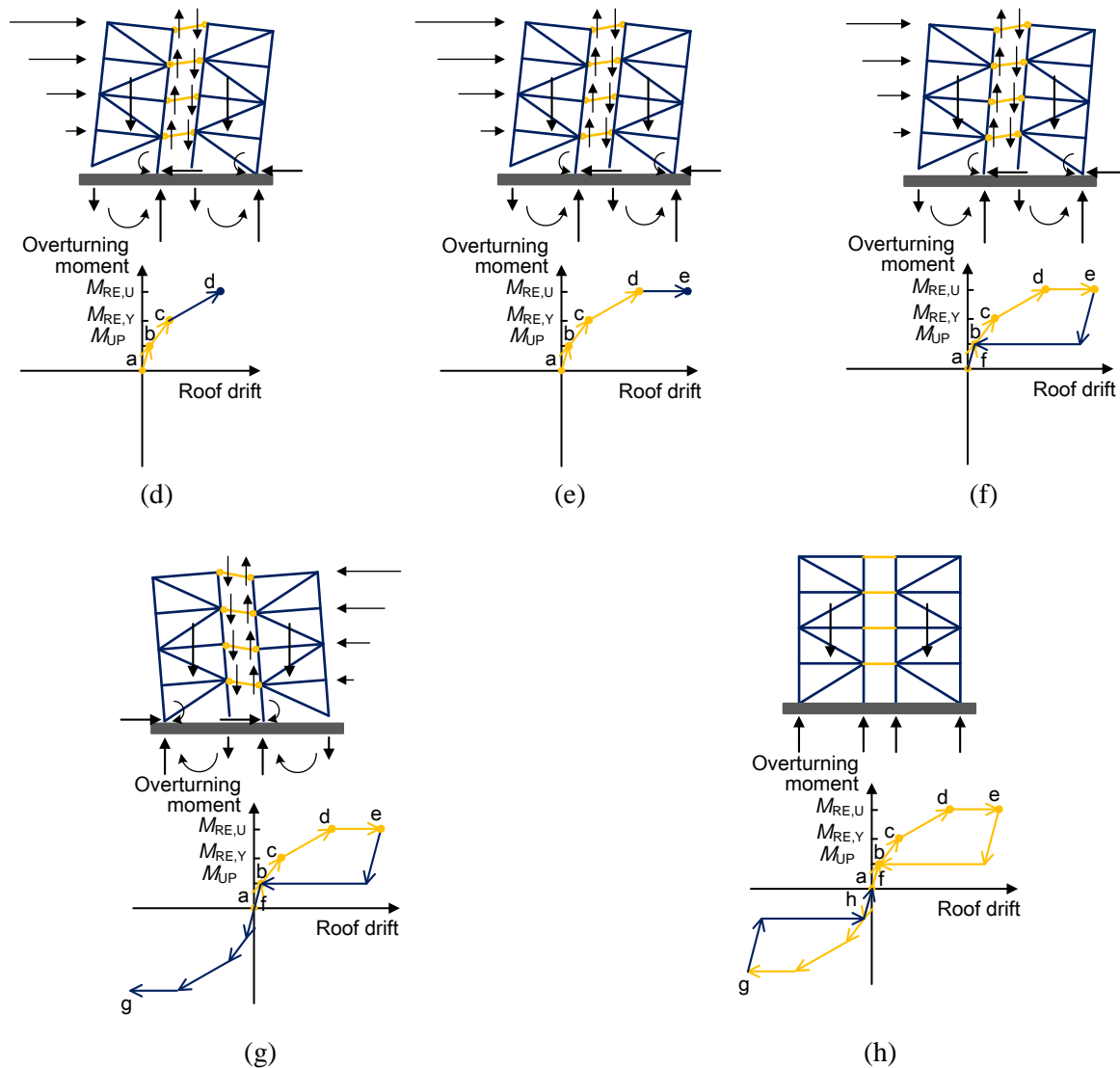


Fig. 2 –Hysteretic behavior of the DLRF: (a) At rest; (b) Uplift; (c) Yielding of ductile links; (d) Yielding of rocking column bases; (e) Maximum displacement; (f) Unloading; (g) Reward loading; (h) At rest

2.2 Performance Objectives

The DLRF is targeted to achieve higher performance than the code-compliant steel frame thus more stringent displacement and acceleration limits will be adopted. The limit states of the DLRF and whether they are permitted at the immediate occupancy (IO), rapid return (RR) or collapse prevention (CP) performance levels are summarized in Table 1.

From the service level earthquake (SLE, with a probability of exceedance of 63% in 50 years) to DBE, all the structural elements remain elastic and the DLRF reaches the IO level, accompanied by the onset of rocking. From the DBE to the maximum considered earthquake (MCE, with a probability of exceedance of 2% in 50 years), yielding of the ductile links is observed during this stage and the RR level is achieved. As exceeding the MCE and even up to the very rare earthquake (VRE, with a probability of exceedance of 0.5% in 50 years), the rocking column bases begin to yield while the rocking steel braced frame elements still remain elastic, and thereby intending to achieve CP level. The alternative performance objectives for the DLRF under various levels, Δ_{ly} and Δ_{by} , could be satisfied without changing the following design methodology. In addition, the associated overturning moment-roof drift relationship of the DLRF is illustrated in Fig. 3.



Table 1 –Limit states and performance objectives

Limit state	IO	RR	CP
Uplift	Yes	Yes	Yes
Yielding of ductile links (Peak roof drift > Δ_{ly})	No	Yes	Yes
Yielding of rocking column bases (Peak roof drift > Δ_{by})	No	No	Yes
Yielding of steel frame elements	No	No	No
Overturning	No	No	No

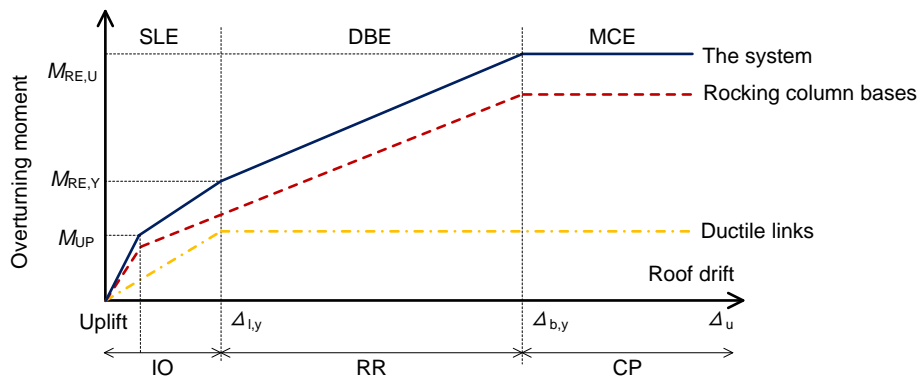


Fig. 3 – Overturning moment-roof drift relationship of the DLRF

3. Capacity Design Procedure of the DLRF

3.1 Overturning moment

For low- to medium-rise buildings, the effects of higher modes on a building can be neglected and the behavior of the rocking steel frame is dominated by the rigid body rotation. Therefore, it is assumed that the response of the DLRF is controlled by the first-mode, and thereby the design base shear is calculated in accordance with the Chinese code for seismic design of buildings [14]. The design base shear distributes up the frame height with a pattern of an inverse-triangle distribution. Therefore, the overturning moment applied to the DLRF, M_{OT} , can be determined as follows

$$M_{OT} = \sum F_i H_i \quad (1)$$

Where F_i is the horizontal seismic load of level i corresponding to different ground motion intensities; H_i is the height of level i above the base.

With reference to the preceding discussion about the overturning moment-roof drift relationship of the DLRF, the overturning moment resistance is calculated as

$$M_{RE} = M_W + M_{DL} + M_{RB} \quad (2)$$



Where M_W is the moment resistance provided by the corresponding gravity load tributary to the DLRF; M_{DL} is the moment resistance provided by the ductile links; M_{RB} is the moment resistance provided by the rocking column bases.

For consistency with the design provisions, the provided moment resistance should exceed the code-compliant overturning moment, that is,

$$M_{RE} \geq M_{OT} \quad (3)$$

3.2 Uplift

As previously mentioned, the behavior of the DLRF is identical to that of the traditional steel braced frame before uplift occurs. Once the distributed gravity load is overcome, the column bottom on one side of the rocking steel braced frames is separated from the foundation and the steel braced frames begin to rock, as shown in Fig. 4(a). Then the uplift moment M_{UP} is determined as

$$M_{UP} = M_W \quad (4)$$

$$M_W = WL_B/2 \quad (5)$$

Where W is the gravity load tributary to the DLRF; L_B is the distance from the uplift column to the rocking pivot point.

3.3 Yielding of ductile links

Referring to the performance objectives of the DLRF discussed previously, the yield moment resistance $M_{RE,Y}$ of the DLRF is reached as yielding of the ductile links occurs under the DBE. It can be seen that the two rocking steel braced frames rock around their respective rocking pivot points, the associated resistance mechanism of the DLRF is illustrated in Fig. 4(b). In that state, the contribution of rocking column bases is neglected for conservation. As a result, the corresponding moment resistance consists of the gravity load and ductile links, as outlined in Eq. (7). Moreover, it is assumed that the ductile links along the height of the building reach their yield strength at the same time. Then the required yield strength of the cross-section of the ductile link $M_{link,y}$ is given in Eq. (8).

$$\sum F_{LY,i}H_i = M_{RE,Y} \quad (6)$$

$$M_{RE,Y} = M_W + M_{DL,Y} \quad (7)$$

$$M_{DL,Y} = \sum M_{link,y} \quad (8)$$

Where $F_{LY,i}$ is the corresponding inverted triangular loads under the DBE; $M_{DL,Y}$ is the total required moment resistance of the ductile links.

3.4 Yielding of rocking column bases

The following event is the yielding of the rocking column bases under the MCE. The corresponding moment resistance subjected by the DLRF is defined as the maximum moment, $M_{RE,U}$. The associated resistance mechanism of the DLRF during this stage is shown in Fig. 4(c). The moment resistance provided by the ductile links has been obtained in the previous step. In terms of the rocking column base, there are two moment resistance mechanisms. When the axial force is compression force, the moment resistance is determined by the configuration of the column base, which could be selected with reference to Cui *et al.* [15]. When the axial force is tension force, the moment resistance is the product of the associated axial force and the distance relative to the rocking pivot point. The associated axial force is also determined by the configuration of the column



base. Then the yield moment resistances of the rocking column base in tension and compression force, $M_{RB,CY}$ and $M_{RB,TY}$, are expressed as Eq. (11) and Eq. (12), respectively.

$$\sum F_{LU,i}H_i = M_{RE,U} \quad (9)$$

$$M_{RE,U} = M_w + M_{DL,Y} + M_{RB,CY} + M_{RB,TY} \quad (10)$$

$$M_{RB,CY} = n_c \left(T_y d + N_c \frac{d}{2} \right) \quad (11)$$

$$M_{RB,TY} = n_t \alpha T_y L_B \quad (12)$$

where $F_{LU,i}$ is the associated inverted triangular loads under the MCE; $M_{RB,CY}$ is the total required moment resistance of the rocking column bases in compression; n_c is the number of the rocking column bases in compression; T_y is the yield force of the anchor rods in tension for one rocking column base; N_c is compressive axial load applied on the rocking column base, which is assumed to be half of the gravity load of the DLRF in the preliminary design, $N_c = W/2$; d is the length of the base plate along the direction of the lateral force, which is determined by the configuration of the column base; $M_{RB,TY}$ is the total required moment resistance of the rocking column bases in tension; n_t is the number of the rocking column bases in tension; αT_y is the total yield force of the anchor rods in tension for one rocking column base, α could be selected as 2 in the preliminary design by considering the symmetry of the configuration.

3.5 Elements of rocking steel braced frame

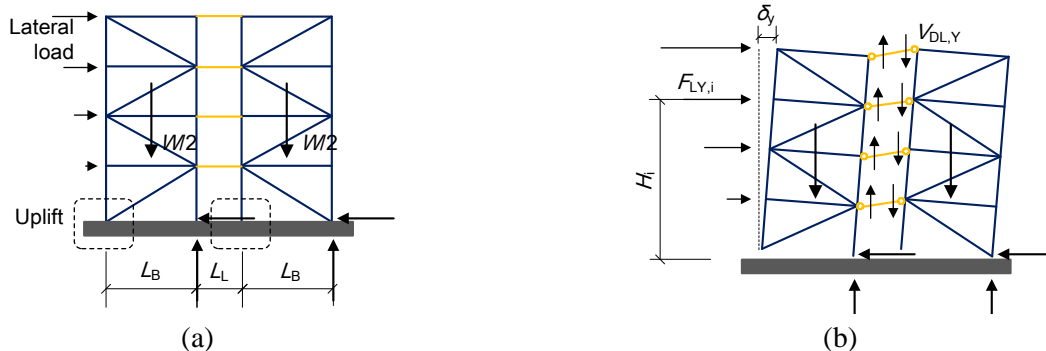
It is expected that the seismic damage of the DLRF is only concentrated in the ductile links and rocking column bases under the MCE, while the structural members of the steel braced frames remain essentially elastic. After the sizes of the ductile links and rocking column bases have been selected, the steel braced frame members could be designed to remain elastic under the largest forces generated by the energy dissipation devices. The corresponding design free body diagram of the steel braced frame is shown in Fig. 4(d). The maximum moment resistances of the ductile links and rocking column bases are expressed as follows, respectively.

$$M_{link,u} = \omega M_{link,y} \quad (13)$$

$$M_{cb,cu} = \beta M_{cb,cy} \quad (14)$$

$$M_{cb,tu} = \gamma M_{cb,ty} \quad (15)$$

where ω is the strength hardening adjustment factor of ductile links, which is the ratio of maximum strength divided by the expected yield strength; β and γ are the compression and tension strength hardening adjustment factors of rocking column bases, respectively, which are defined as the ratio of the maximum moment resistance divided by the yield moment resistance.



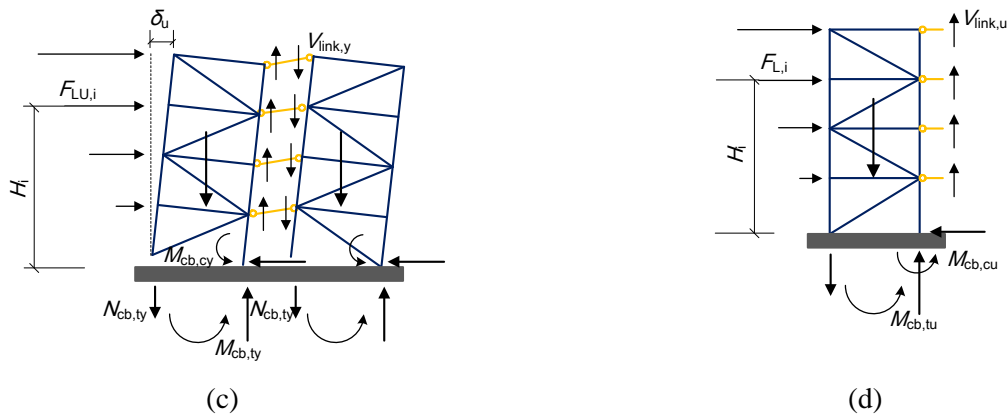


Fig. 4 – Resistance mechanisms of the DLRF under various stages: (a) Uplift; (b) Yielding of ductile links; (c) Yielding of rocking column bases; (d) Free body diagram of rocking steel braced frame for design

4. Case study

4.1 Prototype frame design

The design concepts and procedures presented above are investigated by application to a 4-story prototype residential building located in Beijing, China. The floor plan of the building and a typical elevation of the DLRF are illustrated in Fig. 5. The seismic force-resisting system in the longitudinal direction is moment-resisting frames, only the transverse direction is described in this DLRF example. The building has a plan dimension of 41.6 m × 12.1 m and a total height of 12 m. The rocking steel braced frame has a span of 4.8 m and a centerline column spacing of 2.5 m between the two rocking steel braced frames.

The prototype building is in a highly seismic region with the site of Site Class II and the characteristic period of the seismic response spectra is 0.40 s, as described in [14]. The DLRF is designed to satisfy the demand of the DBE, which has a peak ground motion of 0.2g. The amplitudes of the MCE design spectra is 2 times that of the DBE design spectrum. In addition, Q355 (nominal yield stress f_y is 355 MPa) steel is used for all structural members, including columns, beams, braces, and ductile links. The corresponding member sizes are illustrated in Fig. 5. In accordance with the GB50011-2010 [14], the peak drift ratios of the four-story steel frame under DBE and MCE are selected as 0.5% and 1.0%, respectively.

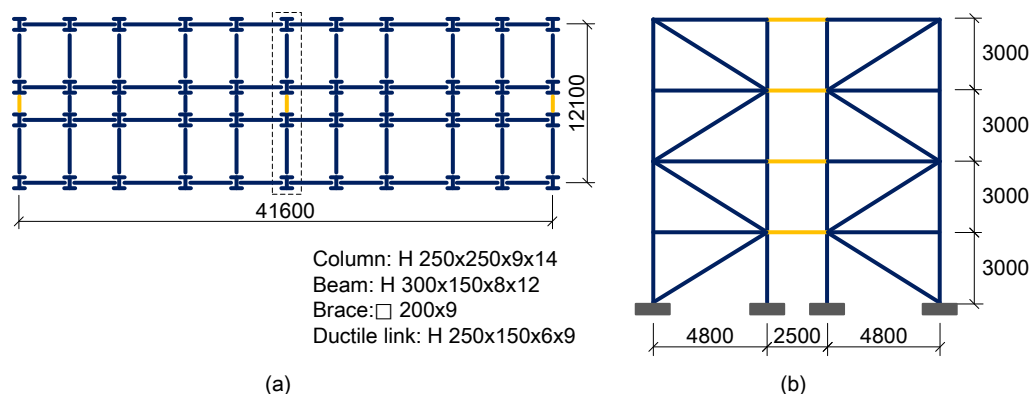


Fig. 5 – Prototype building (unit: mm): (a) Floor plan; (b) Typical elevation of the DLRF

4.2 Validation of the method through nonlinear static analysis

A two-dimensional model was developed using SAP2000 [16], along with the idealized model shown in Fig. 6. Concentrated plasticity models were used for all structural elements, including columns, beams, braces, and



ductile links. At the base of the frame, the horizontal displacement was fixed to transfer the shear force, the uplift and recenter due to rocking were modeled by combining a gap link and an elastic link in parallel in the vertical direction, accompanied by a rotational damper-friction link to capture the self-centering behavior.

Following the required moment resistance of the rocking column base described in the previous section, the corresponding configuration of the rocking column base was determined and thus the values for defining the associated parameters of the links in the model were obtained. Assuming that the four rocking column bases share the identical configuration. The stiffness of the gap link was estimated as 1×10^6 N/mm, equal to the compressive stiffness of the associated reinforced concrete foundation. It is noticeable that the elastic link in the vertical direction is used to avoid ill-conditioned stiffness matrices, which has relatively small stiffness equal to 0.01 times that of the gap link. In terms of the rotational damper-friction link, the initial stiffness was approximately 1×10^{11} Nmm/rad.

The nonlinear pushover analysis was carried out to verify the occurrence of the limit states and evaluate the lateral response of the DLRF. The node at the top of the structure was selected as the monitoring point and the target displacement was 3% of the height of the building (360 mm), as shown in Fig. 6(a). For comparison, a fixed-base structure model was created, in which all structural components and the corresponding material were the same as those in the rocking structure model, except for the base of the frame that was fixed in the model. Consequently, the fundamental periods of the rocking structure and the corresponding fixed-base structure from the modal analyses were 0.254 s and 0.229 s, respectively.

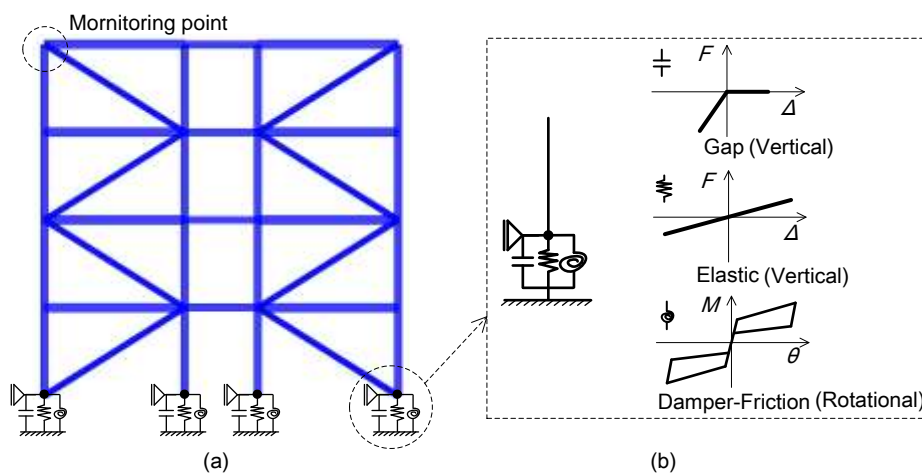


Fig. 6 – Schematic of the numerical model in SAP2000: (a) Frame model; (b) Rocking column base model

The pushover responses of the rocking structure and the fixed-base structure are compared in Fig. 7, along with the limit states and the corresponding plastic hinges distribution of the DLRF. The comparison of the rocking structure and the fixed-base structure indicated that there was no significant difference until the uplift occurred. It is obvious that the fixed-base structure exhibits extremely high lateral resistance at the cost of poor ductility.

In terms of the rocking structure, three limit states were found as expected. The column bottom began to separate from the foundation at a roof drift of approximately 0.06%, followed by the yielding of the ductile links and yielding of the rocking column bases as the lateral load increased. The associated roof drifts were around 0.56% and 1.0% along with changes in the lateral stiffness, respectively. In the end, the analysis was terminated at a roof drift of 3.0%. It was particularly noticeable that the plasticity was only confined to the ductile links, indicating that the steel braced frames motion is dominated by rigid body rotation. Therefore, the DLRF's ability to damage control and prediction of the frame was demonstrated.

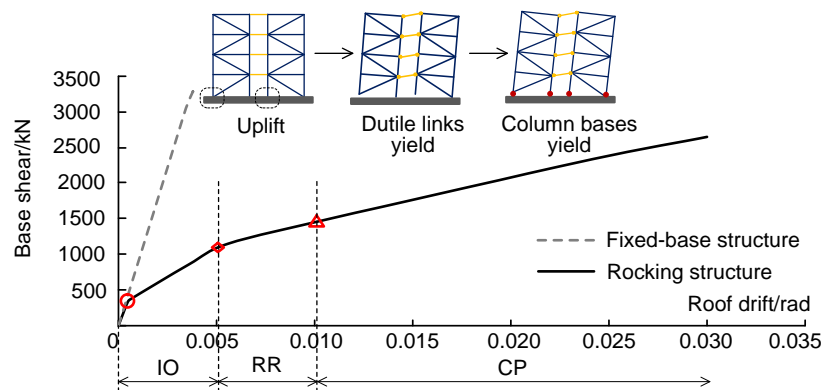


Fig. 7 – Pushover responses of the rocking structure and fixed-base structure

5. Conclusions

- (1) An innovative lateral force-resisting system called ductile linked rocking steel frames (DLRF) was introduced and investigated in this paper. The overturning moment versus roof drift relationship of the DLRF under lateral loads was illustrated in various stages, together with the corresponding limit states.
- (2) The gravity load is overcome and the column bottom begins to uplift from the SLE to DBE intensities, yielding of the ductile links is observed under the DBE intensity followed by yielding of the rocking column bases under the MCE intensity.
- (3) The design procedure to describe the overturning moment-roof drift under various ground motion intensities were established. Based on the results of the nonlinear static analyses, this paper showed that the DLRF designed in accordance with the proposed equations can capture the targeted limit states as desired.

6. References

- [1] Architectural Institute of Japan (AIJ) (2011): *Preliminary Reconnaissance Report of the 2011 Tohoku-Chiho Taiheiyō-Oki Earthquake*. Japan. (in Japanese)
- [2] Comerio M, Elwood K, Berkowitz R (2011): *The M6.3 Christchurch, New Zealand, earthquake of February 22, 2011*. Oakland: Earthquake Engineering Research Institute (EERI).
- [3] Housner GW (1963): The behavior of inverted pendulum structures during earthquakes. *Bulletin of the Seismological Society of America*, **71**(2), 403-417.
- [4] Midorikawa M, Azuhata T, Ishihara T, Wada A (2006): Shaking table tests on seismic response of steel braced frames with column uplift. *Earthquake Engineering Structural Dynamics*, **35**(14), 1767-1785.
- [5] Gledhill SM, Sidwell GK, Bell DK (2008): The damage avoidance design of tall steel frame buildings - Fairlie Terrace student accommodation project. Victoria University of Wellington. *Proc. of 2008 New Zealand Society for Earthquake Engineering (NZSEE) Conference*, Taupo, New Zealand.
- [6] Ramhormozian S, Clifton GC, Beskhyroun S, MacRae GA (2018): Dynamic performance analysis and system identification (SI) of a low damage multi-storey structural steel building under two moderately severe earthquake events using SHM. *2018 New Zealand Society for Earthquake Engineering (NZSEE) Conference*, Auckland, New Zealand.
- [7] Tremblay R, Poirier LP, Bouaanani N, Leclerc M, Rene V, Feonteddu L, Rivest S (2008): Innovative viscously damped rocking braced steel frames. *14th World Conference on Earthquake Engineering*, Beijing, China.
- [8] Roke D, Sause R, Ricles JM, Gonner N (2010): Damage-free seismic resistant self-centering concentrically-braced frames. *ATLSS Report. 10-09*, Lehigh University, Bethlehem, PA.



- [9] Sause R, Rides JM, Roke DA (2010): Seismic Performance of a Self-Centering Rocking Concentrically-Braced Frame. *9th US National and 10th Canadian Conference on Earthquake Engineering*, Toronto, Canada.
- [10] Ma X, Eatherton M, Hajjar JF, Krawinkler H, Deierlein GG (2010): Seismic design and behavior of steel frames with controlled rocking – part II: large scale shake table testing and system collapse analysis. *Structures Congress/North American Steel Construction Conference (NASCC)*, Orlando, Florida, USA.
- [11] Eatherton M, Ma X, Krawinkler H, Deierlein GG, Hajjar JF (2014): Quasi-static cyclic behavior of controlled rocking steel frames. *Journal of Structural Engineering*, **140**(11), 04014083.
- [12] Wiebe L, Christopoulos C (2015): Performance-based seismic design of controlled rocking steel braced frames. I: methodological framework and design of base rocking joint. *Journal of Structural Engineering*, **141**(9), 04014226.
- [13] Martin A, Deierlein GG, Ma X (2019): Capacity design procedure for rocking braced frames using modified modal superposition method. *Journal of Structural Engineering*, **145**(6), 04019041.
- [14] GB 50010-2010 (2010): *Code for Seismic Design of Buildings*. China Architecture & Building Press, Beijing, China. (in Chinese)
- [15] Cui Y, He YZ, Wang FZ, Li H (2019): Finite element analysis of value-added exposed column base connections. *10th International Symposium on Steel Structures*, Jeju, Korea.
- [16] CSI. SAP2000 (2010): *Integrated Software for Structural Analysis and Design*. Computer & Structures, Berkeley, CA, USA.